Final Draft
of the original manuscript:

Zheng, X.; Dogan, B.; Lorenz, U.; Oehring, M.:
Microstructural Stability and Creep Cracking in Ti6242 Alloys
In: Xiyou Jinshu Cailiao Yu Gongcheng / Rare Metal Materials and Engineering
(2006) Nonferrous Metals Society
2006 Vol. 35(1): 164-167

DOI: -

Microstructural Stability and Creep Cracking in Ti6242 Alloys

X. Zheng[1, 2], B. Dogan[1], U. Lorenz[1] and M. Oehring[1]

1. GKSS Research Centre, Max-Planck-Str.1, D-21502 Geesthacht, Germany

2. Beijing Institute of Technology, Beijing 100081, P.R.China

Abstract: A detailed metallographic study of both as-received and creep tested specimens was carried out on Ti-6242 with equiaxed and lamellar microstructures. It was aimed at a better understanding of micro-mechanisms of creep damage, microstructural instability effects on creep crack behavior. Present investigations demonstrated that the dominant micromechanism controlling slow creep crack growth involves the formation of microstructural damage zones ahead of the crack tip leading to the nucleation and growth of a number of cavities/cracks at α grain/subgrain boundaries. The decomposition of metastable β phase and dissolution of interface phase at α/β boundaries during creep loading have less effect on the formation of cavity. The comparison of two microstructures is made to interpret the influence of substructures and dislocation activities on the creep crack behavior of Ti-6242.

Keywords: Ti-6242; creep crack growth; lamellar microstructure; equiaxed microstructure
Paper Number: GC-24

1 Introduction

The behavior of materials used in high temperature engineering applications is required to have microstructural stability associated with high creep and fracture resistance. However, the service critical components may be exposed to damage leading to creep crack initiation and growth. Components operating at elevated temperatures may fail by slow propagation of a pre-existing macro-crack growing at lower stresses where applied stress intensity factor much lower than those determined by the fracture toughness testing. Therefore, a thorough knowledge of the crack growth behavior and physical mechanisms involving creep is required for assessment of high temperature service behavior of both conventional and new advanced creep-resistant alloys.

Currently used high temperature alloy, Ti-6242, is an important alloy for aeroengine applications with an outstanding combination of strength, toughness and creep resistance. The major phases in this alloy are α with microstructure described as a near α alloy. Various microstructures ranging from lamellar to duplex and equiaxed α can be produced by hot processing and heat treatment.

The tensile and creep deformation behavior, and crack growth of Ti-6242 alloy at room temperature under cyclic loading conditions have been intensively investigated[1~9]. However, less work has been reported on the crack initiation and propagation under creep conditions. The microstructure damage evolution ahead of a creep crack tip in this alloy is less understood. The relationship between microstructral instability and creep damage has not been fully elucidated.

The present paper reports on the detailed metallographic investigations on both as-received material and tested compact tension, C(T) type fracture mechanics specimens of Ti-6242 with equiaxed and lamellar microstructures at 500°C. The microstructural results on the fracture mechanics specimens are discussed in the light of earlier time dependent fracture mechanics studies[10]. Therefore,

the reported work aims at contributing to a better understanding of the microstructural stability and creep damage mechanisms involved in creep crack initiation and growth of Ti6242 alloys.

2 Experimental

The Ti6242 materials used in this study were received in the form of forged discs of 200mm and 220mm in diameter, and in two microstructures designated hereafter as microstructures lamellar and equiaxed or materials A and B. The chemical compositions of the materials are given in Table 1.

Compact tension, C(T) type fracture mechanics specimen of 50mm width and 25mm thickness was machined out of the as-received discs. The specimen with lamellar microstructure was pre-cracked by electric discharge machining (EDM) and creep crack growth tests was performed at 500°C under constant loads of 25KN for 427 hours. The specimen with equiaxed microstructure was pre-cracked by fatigue resulting in 25mm in length and the creep crack growth test was conducted at 500°C under constant loads of 15kN for 1390 hours. Both specimens were interrupted before final fracture in order to determine the final crack length for time dependent fracture mechanics data assessment as well as avoiding final fracture with increased plastic deformation.

Table 1 Chemical composition of Ti6242(wt%)

Element	Material A (Lamellar)	Material B (equiaxed)
Ti	Balance	Balance
Al	6.00	5.98
Mo	1.90	1.88
Zr	4.30	4.21
Sn	2.00	1.99
Si	0.08	0.08
Fe	0.05	0.04
N	0.008	0.009
C	0.013	<0.02
H	0.00519-0.0062	0.0019-0.0091
O	0.080	0.092

After testing, the specimens were sectioned in the mid-thickness through the main crack plane into two pieces. The side surface of one piece was ground and polished and another half was broken by cyclic loading at room temperature to observe the fracture surface. The polished side surfaces and broken fracture surfaces were examined under SEM coupled with EDX. TEM specimens were machined from tested specimens near to the crack tip and then ground and finally thinned by TWIN-JET polishing equipment. The thin foils were examined in a Philips CM200 transmission electron microscope at 200kV.

3 Results and Discussion

3.1 Microstructure development during creep crack growth

The material A has an as cast and forged near lamellar microstructure with elongated α-grains separated by thin pancake shaped β phase. A lamellar packet contains lamellar α grains aligned nearly in the same direction. The material B has a predominately equiaxed α microstructure in a transformed β matrix with small amount of coarse α platelets and fine structure of needle like α platelets. There is no evidence of fine α platelets in lamellar microstructure.

SEM observations show that the individual equiaxed or elongated α grains extending over large areas in both initial microstructures actually consist of small irregular α grains in different orientations with smooth boundary between them as observed in TEM studies. High density of dislocations observed in equiaxed microstructure were homogenously distributed within individual α grains structure and mostly tangled and arranged in hexagonal or rhombic networks by three or two intersecting families of dislocations (Fig.1(a)). Lower dislocation density was observed in lamellar structure and some lamellar α grains consist of subgrains with dislocation boundaries.

The morphology of two microstructures after long time creep exposure at 500°C was similar to those in the initial microstructures. However, much more fine acicular α platelets were formed in prior β matrix visible only at high magnification leading to all β laths or "islands" becoming fragmented into small domains (Fig.2(a)). The decomposition of residual β phase occurred throughout the whole specimen but

accelerated in the vicinity of the crack tip due to deformation leading to higher strains. The partial decomposition of β phase indicates that the equilibrium volume fractions of the phases were not achieved in initial materials. This also points out

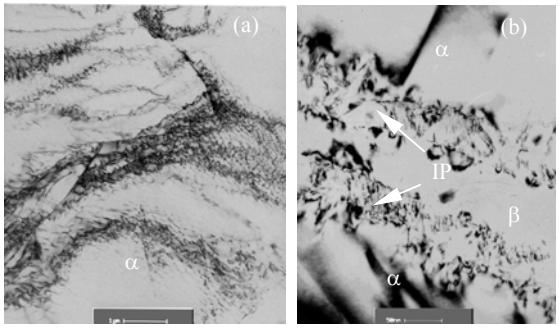

Fig.1 TEM micrographs showing (a) dislocations in as-recieved equiaxed structure and (b) the interface phase (IP) in as-received lamellar structure

instability of the studied microstructures.

The transition zone at α/β interfaces present in as-received lamellar structure, as shown in Fig.1(b) has similar morphology to that designated as an interface phase with fcc or hcp crystal structures in some reports[11, 12]. The formation of interface phase was thought to be an artifact which occurs when specimen absorbs hydrogen during electro-polishing. However, our observation indicates that the interface phase was not evident at α/β interfaces in both tested CT specimens and dislocations emanating wave-like from α/β interface were observed in α phase near α/β interfaces in lamellar structure. It was suggested to be stress induced with high density of dislocations during cooling from high temperatures to accommodate the lattice mismatch between α and β phase. A much higher dislocation density and more dislocation tangles in α grains of CT specimens with lamellar structure may be attributed to the liberation of these dislocations from the α/β interface which may provide a source for creep by slipping [8], and on the other hand, the considerable stress concentration may arise in these regions containing high density dislocations if the movement of these dislocations is difficult when the orientation of lamellar colony is not favorable for deformation with respect to the loading axis hence resulting stress. This will lead to the early formation and propagation of voids or cracks in these regions during creep. This is possibly an important observation that contributes to the relative lower creep crack resistance in lamellar structure, compared with equiaxed structure.

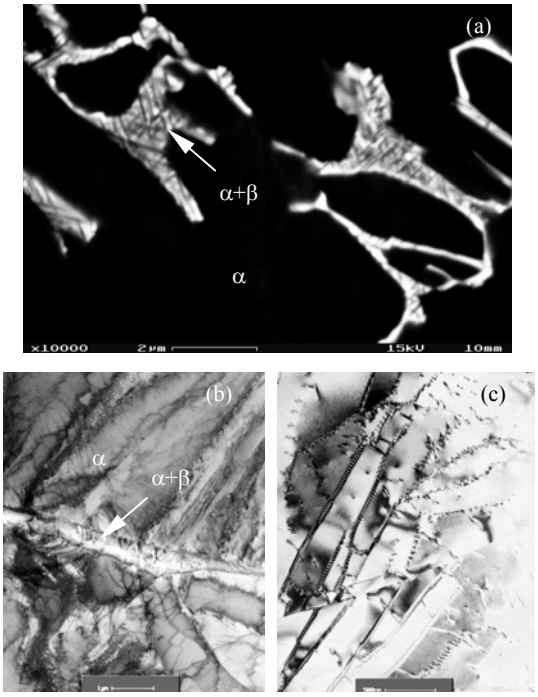

Fig.2 (a) SEM micrograph of the decomposition of residual β phase in equiaxed structure, (b) and (c) TEM micrographs showing high dislocation density and dislocation networks in lamellar structure after long term creep exposure

The high density of dislocations in CT specimens led to the formation of more subgrains and dislocation cells with smaller size and well-defined dislocation networks or walls (tangles) (Fig.2(b)). Some networks oriented themselves in certain crystallographic directions and surrounding regions are almost free from dislocations (Fig.2(c)), implying extensively dislocation slipping by multiple slip systems activity and flowed by dislocation climb with recovery occurred during creep exposure.

No apparent dislocations were visible within β grains in both as-received and tested specimens after long time creep exposure in two microstructures in agreement with previous reports[8, 9], demonstrating that the creep deformation and fracture in this alloy is largely dominated by the movement of dislocations by the slipping and climbing within α grains.

Silicides were not found in two CT specimens after

long time exposure at 500°C as the content of silicon in this alloy is relative low. No evidence shows the recrystallization of α grains even nearest to the crack tip. Note that well-defined dislocation networks indicates only recovery with the dislocation climb during creep crack growth.

3.2 Creep crack growth and damage zone development

SEM micrograph in Figure 3 clearly shows slow creep crack growth with crack branching observed on the sectioned side surface of the CT specimen with equiaxed microstructure after period of long time loading at 500°C. The two short creep cracks extended from pre-existing crack–root and propagated symmetrically oriented about 40° from the initial notch plane. The deflected crack paths indicate creep crack initiation and growth controlled by the local stresses ahead of the crack tip flowing active deformation planes aligned along slip field lines with underlying microstructures.

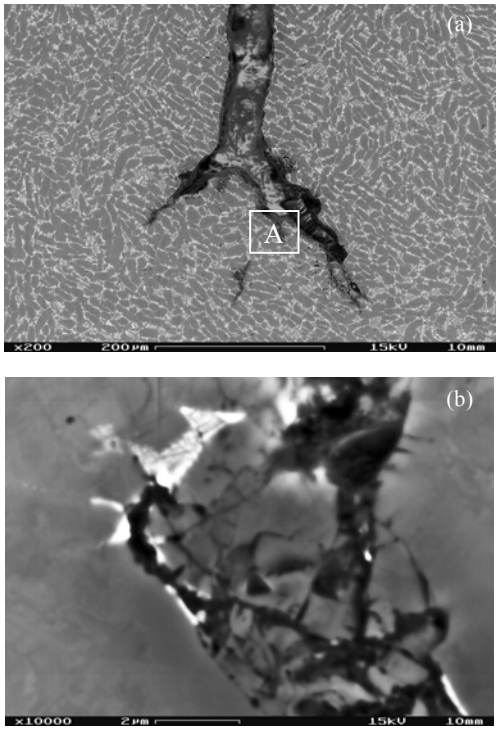

Fig.3 SEM microsgraphs of (a) the creep crack and (b) Enlarged image of area "A" in (a) showing creep damage in the CT specimen with equiaxed structure

The creep damage bands developed across the α grains ahead of the crack tip were observed on both sides. High magnification observations revealed that very fine voids and cracks were formed mostly within primary equiaxed α grains in the vicinity of the creep crack tip. The formation of micro-cracks at the crack tip is considered to arise from stress concentration at α grain/subgrain boundaries. The voids nucleate and grow at α grain/subgrain boundaries to form microcracks of network and subsequent linkage of microcracks leads to a primary α grains broken up to pieces. The long cracks along the coarse α grain boundary or across the transformed β matrix can be observed in front of the creep damage bands. Much less cavities were observed in partially transformed β matrix and at α/β interfaces, indicating the transformation of metastable β to fine α platelets and liberation of dislocations from the α/β interface during creep process favor the release of the stress

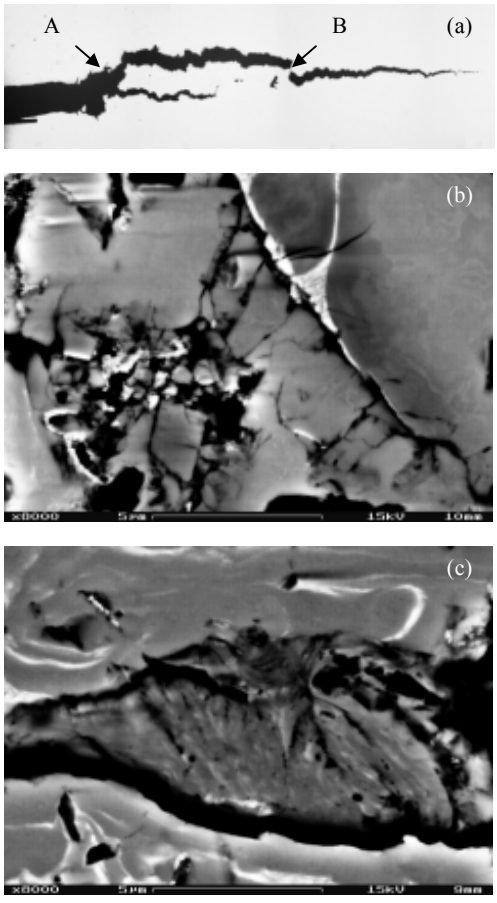

Fig.4 (a) OM micrograph of the creep crack and SEM micrographs showing creep damage, (b) enlarged image of area "A" in (a) showing creep damage in slow crack growth regime and (c) enlarged image of area "B" in (a) showing creep damage in fast crack growth regime in CT specimen with lamellar microstructure.

during creep crack growth.

Extensive micro-deformation was evident only in α grains near the crack tip resulted from the interaction of high stress concentration with local microstructures. No macro-deformation bands could be seen in the vicinity of the crack tip, indicating the limited creep deformation in this alloy under the present creep crack growth conditions.

Optical image in Fig.4(a) shows creep cracks propagated in a nearly straight line being non-coplanar with the initial crack plane in the specimen with lamellar microstructure. The creep crack growth is much fast comparing with equiaxed microstructure due to higher load applied and relative low creep crack growth resistance for lamellar structure [10].

The similar damage bands along the early creep crack growth path (slow growth regime) in lamerllar microstructure were also observed, as shown in figure 4(b). It is evident that the slow creep crack propagation in lamellar structure is also through the formation of damage zones with the size comparable to α grain size arising from the initiation and coalescence of cavities at the α grain/subgrain boundaries. However, the microstructural damage in fast crack growth was resulted from the heavy slipping and followed by the formation of cavities on both slipping planes and partially transformed β areas as shown in figure4(c), indicating less recovery process and different damage mechanism including plastic deformation.

It is obvious that the main creep crack propagation was directly related to the formation of dislocation networks. The sub-grain boundaries with low energy blocked the motion of dislocations and gliding of boundaries and provided the sites for the high strain concentration.

4 Conclusions

The detailed microscope study on both as-received and creep tested specimens of Ti6242 with equiaxed and lamellar microstructures provided information on the creep crack growth by the initiation of cavities at subgrain boundaries and subsequent coalescence of cavities to form damage zones. The microstructural changes occurred in both two microstructural conditions. TEM examination demonstrated the stable dislocation networks present within initial lamellar and equiaxed α grains being suggested to accounts for the microstructure damage during creep crack growth. Higher creep resistance and creep crack growth rate of lamellar microstructure may be related to the initial lower dislocation density and more dislocation activities limitation within lamellar α grains due to the liberation of dislocations from α/β interfaces. The decomposition of metastable β phase and dissolution of the interface phase which have less effect on the formation of cavity in the slow creep crack growth regime.

Acknowledgement:

The assistance given during the course of the presented work by U.Ceyhan, V.Ventzke of GKSS is gratefully acknowledged

References

[1] Hayes R W *et al. Acta Materialia*[J], 2002, 50:4953~4963.

[2] Neeraj T *et al. Acta Materialia*[J], 2000, 48:1225~1228.

[3] Jin O, Mall S. *Materials Science and Engineering*[J], 2003, A359:356~367.

[4] Es-Souni M. *Materials Characterization*[J], 2000, 45:153-164.

[5] Sansoz F, Ghonem. *Materials Science and Engineering*[J], 2003, A00:1~12.

[6] Viswanathan G B *et al*. *Materials Science and Engineering*[J], 2001, A319-321:706~710.

[7] Srivatsan T S *et al. Materials Science and Engineering*[J], 2002, A334:327~333.

[8] Viswanathan G B *et al*. *Acta Materialia*[J], 2002, 50:4965~4980.

[9] Bourgeois M *et al*. Titanium‘ 95 Science and Technology. Cambridge, The University Press, 1996:1083~1090.

[10] Dogan B *et al*. *Materials at High Temperatures*[J], 1992, 10:138~143.

[11] Banerjee D *et al*. Titanium Science and Technology. Oberursel, Germany: Deutsche Gesellschaft fur Metallkunde, 1985:1597~1604.

[12] Murakami Y. Titanium‘ 80 Science and Technology. Warrendale, PA: AIME, 1981: 153~167.